The Journal of Experimental Biology 203, 2297–2310 (2000)
Printed in Great Britain © The Company of Biologists Limited 2000
JEB2681

IMMUNOLOCALIZATION OF ION-TRANSPORT PROTEINS TO BRANCHIAL EPITHELIUM MITOCHONDRIA-RICH CELLS IN THE MUDSKIPPER (*PERIOPHTHALMODON SCHLOSSERI*)

JONATHAN M. WILSON[1,*], DAVID J. RANDALL[1], MARK DONOWITZ[2], A. WAYNE VOGL[3] AND ALEX K.-Y. IP[4]

[1]*Department of Zoology, University of British Columbia, Vancouver, Canada V6T 1Z4,* [2]*Departments of Medicine and Physiology, GI Unit, Johns Hopkins University, Baltimore MD 21205-2195, USA,* [3]*Department of Anatomy, University of British Columbia, Vancouver, Canada V6T 1Z3* and [4]*Department of Biological Sciences, National University of Singapore, Singapore 0511*

*Present address: Centro Interdisciplinar de Investigação Marinho e Ambiental (CIIMAR), Rua do Campo Alegre 823, 4150-180 Porto, Portugal (e-mail: wilson_jm@cimar.org)

Accepted 26 April; published on WWW 10 July 2000

Summary

The branchial epithelium of the mudskipper *Periophthalmodon schlosseri* is densely packed with mitochondria-rich (MR) cells. This species of mudskipper is also able to eliminate ammonia against large inward gradients and to tolerate extremely high environmental ammonia concentrations. To test whether these branchial MR cells are the sites of active ammonia elimination, we used an immunological approach to localize ion-transport proteins that have been shown pharmacologically to be involved in the elimination of NH_4^+ (Na^+/NH_4^+ exchanger and Na^+/NH_4^+-ATPase). We also investigated the role of carbonic anhydrase and boundary-layer pH effects in ammonia elimination by using the carbonic anhydrase inhibitor acetazolamide and by buffering the bath water with Hepes, respectively. In the branchial epithelium, Na^+/H^+ exchangers (both NHE2- and NHE3-like isoforms), a cystic fibrosis transmembrane regulator (CFTR)-like anion channel, a vacuolar-type H^+-ATPase (V-ATPase) and carbonic anhydrase immunoreactivity are associated with the apical crypt region of MR cells. Associated with the MR cell basolateral membrane and tubular system are the Na^+/K^+-ATPase and a $Na^+/K^+/2Cl^-$ cotransporter. A proportion of the ammonia eliminated by *P. schlosseri* involves carbonic anhydrase activity and is not dependent on boundary-layer pH effects. The apical CFTR-like anion channel may be serving as a HCO_3^- channel accounting for the acid–base neutral effects observed with net ammonia efflux inhibition.

Key words: mudskipper, *Periophthalmodon schlosseri*, ammonia, excretion, mitochondria-rich cell, gill, Na^+/H^+ exchange, Na^+/K^+-ATPase, CFTR, $Na^+/K^+/2Cl^-$ cotransport, carbonic anhydrase, H^+-ATPase.

Introduction

The mudskipper *Periophthalmodon schlosseri* is an amphibious, obligate air-breathing, teleost fish with the ability to eliminate ammonia actively (Randall et al., 1999). It is an active carnivore with a high terrestrial affinity, inhabiting the brackish-water mangrove swamps and mudflats of southeast Asia (Murdy, 1989). Related to its ability to excrete ammonia actively is the high tolerance of this species of mudskipper to environmental ammonia (Peng et al., 1998).

P. schlosseri has a 96 h LC_{50} value of 514 μmol l^{-1} NH_3 (Peng et al., 1998) and has an ammonia tolerance similar to that of the equally impressive Lake Magadi tilapia (*Oreochromis alcalicus grahami*; Randall et al., 1989) and the air-breathing catfish *Heteropneustes fossilis* (Saha and Ratha, 1990). However, these species make use of the ornithine–urea cycle to produce urea as a means of detoxifying ammonia, while this mudskipper species does not (Peng et al., 1998). Mudskippers make use of free amino acids and have a powerful glutamate dehydrogenase/glutamine synthetase system for ammonia detoxification in the brain (Iwata, 1988; Peng et al., 1998). Incidentally, the ammonia levels in the burrow water of the mudskipper have been measured at 2 mmol l^{-1} (Y.-K. Ip, unpublished observations). Also, when out of water, *P. schlosseri* remain ammoniotelic, increasing ammonia, urea and free amino acid stores (Ip et al., 1993) and excreting the remainder into the boundary layer of water covering the animal (Wilson et al., 1999). Terrestrial excursions by other amphibious teleosts are generally characterized by a loss of the capacity to eliminate ammonia (Morii et al., 1978; Iwata et al., 1981).

Randall et al. (1999) have demonstrated high levels of Na^+/K^+-ATPase activity associated with the gills that can be activated by physiological levels of NH_4^+ instead of K^+. Net

ammonia excretion rates were also sensitive to *in vivo* pharmacological inhibition of Na^+/K^+-ATPase by ouabain and of the Na^+/H^+ exchanger (NHE) by amiloride. Measured transepithelial potentials could not account for ammonia effluxes in high environmental ammonia levels, indicating that ammonia efflux is active.

The branchial epithelium of this species is unique among species of mudskipper and teleost fishes in general (Schöttle, 1931; Low et al., 1988, 1990; Wilson et al., 1999). The lamellar epithelium is densely packed with mitochondria-rich (MR) cells, and the interlamellar water spaces are restricted by interlamellar fusions. The opercular epithelium, which is lined with intraepithelial capillaries, appears to be better suited to gas exchange (Schöttle 1931; Wilson et al., 1999). The branchial MR cells have a tubular system continuous with the basolateral membrane that is typical of teleost fishes (Pisam, 1981; Philpott, 1980). However, the MR cells of this species have deep apical crypts, and accessory-type cells were seldom observed (Wilson et al., 1999). Accessory cells are typically associated with active NaCl elimination in marine teleost fishes. It is this apparent lack of accessory cells and the over-abundance of MR cells that suggest a function in addition to NaCl elimination for the gill population of MR cells. It would appear that the ability of these animals to eliminate ammonia actively is probably associated with the branchial MR cells.

In the present study, we investigate the possibility that the branchial epithelium is the site of active NH_4^+ elimination. Ion-transport proteins involved in the active elimination of NH_4^+ are localized using an immunological approach employing non-homologous antibodies. Antibodies against the following proteins were used: NHE2 and NHE3, the cystic fibrosis transmembrane regulator-like anion channel (CFTR), vacuolar-type H^+-ATPase (V-ATPase), carbonic anhydrase, Na^+/K^+-ATPase and the $Na^+/K^+/2Cl^-$ cotransporter (NKCC). We also investigated the role of carbonic anhydrase in ammonia elimination by using the carbonic anhydrase inhibitor acetazolamide and the role of boundary-layer pH effects by buffering the bath water with Hepes at pH 8.0 and 7.0.

Materials and methods

Animals

Adult *Periophthalmodon schlosseri* (Pall.) of both sexes were collected from the Pasir Ris, a small estuary on the east coast of Singapore, and transported to City University of Hong Kong. In the laboratory, fish in individual plastic aquaria were kept partially submerged in 50 % sea water (salinity 15 ‰). Every second day, the water was changed and the animals were fed goldfish (*Carassius auratus*) *ad libitum*. Fish mass ranged from 55 to 120 g. The room air and water temperatures remained constant at approximately 26 °C. No attempts were made to control lighting conditions, and a natural photoperiod was followed.

Inhibitor studies and Hepes buffering

Animals were fasted for 3 days prior to the start of experimentation. Fish kept in 500 or 1000 ml of 50 % sea water were exposed to a series of three flux periods. An initial 3 h control flux period was followed by a 3 h experimental flux period and finally a 3 h recovery flux period. The experimental exposures consisted of exposing the fish either to 0.1 mmol l^{-1} acetazolamide to inhibit carbonic anhydrase or to 5.0 mmol l^{-1} Hepes to maintain water pH at the gill surface at either pH 7 or pH 8. Control and recovery fluxes were conducted in 50 % sea water. For the first two flux periods, water samples were taken at 0, 1, 2 and 3 h, but water samples were taken only at 0 and 3 h for the recovery period.

Water samples were assayed for total ammonia concentration (Verdouw et al., 1978), from which ammonia flux rates (J_{Amm}) were calculated (μmol ammonia kg^{-1} fish h^{-1}). Appropriate standards were prepared with acetazolamide or Hepes (pH 7 and 8) in 50 % sea water. Titratable acidity (TA) flux (J_{TA}) was measured according to the method of McDonald and Wood (1981) from the difference between 0 and 3 h water samples from the control and experimental periods. In brief, 100 ml water samples were aerated overnight to remove respiratory CO_2, and 25 ml subsamples (weighed to 0.01 g) were titrated to pH 4.00 with 0.01 mol l^{-1} HCl using a Radiometer autotitrator and Orion Ross-type combination electrode. Aeration continued during titration to remove liberated CO_2. The net acid flux (J_{Acid}; μequiv H^+ kg^{-1} h^{-1}) was calculated as the sum of J_{TA} and J_{Amm}, signs considered.

Tissue fixation for immunocytochemistry

Whole gill arches were immersion-fixed for immunolocalization studies at the light microscopic level using 3 % paraformaldehyde/phosphate-buffered saline (PFA/PBS), pH 7.4, and at the electron microscopic level using 2 % paraformaldehyde, 75 mmol l^{-1} L-lysine, 10 mmol l^{-1} sodium *m*-periodate fixative (McLean and Nakane, 1974) overnight at 4 °C. Following fixation in 3 % PFA/PBS, tissues were rinsed in PBS and 10 % sucrose/PBS and either frozen in liquid nitrogen or processed for paraffin embedding (Paraplast, Fisher Scientific). Following fixation for immunoelectron microscopy, tissue was rinsed in PBS, and free aldehyde groups were quenched in a 50 mmol l^{-1} NH_4Cl solution for 20 min. The tissue was then dehydrated through a decreasing temperature (room temperature to −20 °C) ethanol series (1 h each in 30 %, 50 %, 70 %, 95 % and three times for 1 h in 100 % ethanol), gradually infiltrated with resin (ethanol:Unicryl; 2:1, 1:1, 1:2 for 30 min at −20 °C and 100 % Unicryl twice for 1 h and overnight at −20 °C) and transferred to Beem caps for embedding (BioCell International UK). The resin was polymerized using ultraviolet light at −10 °C over 3 days.

Antibodies

Na^+/K^+-ATPase

Gill Na^+/K^+-ATPase was immunolocalized using a monoclonal antibody specific for the α-subunit of chicken Na^+/K^+-ATPase (Takeyasu et al., 1988). The antibody (α5) developed by D. M. Fambrough (Johns Hopkins University, MD, USA) was obtained from the Developmental Studies

Hybridoma Bank maintained by the University of Iowa Department of Biological Sciences, Iowa City, IA 52242, USA, under contract NO1-HD-7-3263 from the National Institute of Child Health and Human Development (NICHD). The antibody was purchased as cell culture supernatant (0.9 mg ml^{-1}). This antibody is now in routine use for identifying gill MR cells by way of their high Na^+/K^+-ATPase levels (Witters et al., 1996; T. H. Lee et al., 1998).

$Na^+/K^+/2Cl^-$ cotransporter (NKCC)

The gill $Na^+/K^+/2Cl^-$ cotransporter was immunolocalized using a monoclonal antibody specific for human colonic NKCC1 (Lytle et al., 1995). The antibody (T4) developed by Christian Lytle (Division of Biomedical Sciences, University of California, Riverside, CA, USA) was obtained from the Developmental Studies Hybridoma Bank maintained by the University of Iowa Department of Biological Sciences, Iowa City, IA 52242, USA, under contract NO1-HD-7-3263 from the NICHD. The antibody was purchased as cell culture supernatant (0.8 mg ml^{-1}). Fixed/frozen dogfish (*Squalus acanthias*) rectal gland tissue was used as a positive control. The T4 monoclonal antibody has greater species cross-reactivity than the J3 monoclonal antibody, the immunoreactivity of which is limited to shark tissues (Lytle et al., 1995).

Na^+/H^+ exchanger (NHE)

Rabbit polyclonal antibodies generated against glutathione S-transferase fusion proteins incorporating the last 87 amino acid residues of NHE2 (antibody 597; Tse et al., 1994) and the last 85 amino acid residues of NHE3 (antibodies 1380 and 1381; Hoogerwerf et al., 1996) were used. Antibody specificity has been determined in NHE-expressing PS120 cell lines. These antibodies have been used in a number of different studies for immunolocalization and western analysis of NHE2 and NHE3 isoforms (He et al., 1997; M. G. Lee et al., 1998; Levine et al., 1993; Sun et al., 1997) including a recent study on two teleost fishes (*Oncorhynchus mykiss* and *Pseudolabrus tetrious*) by Edwards et al. (1999). Three monoclonal antibodies generated against a maltose-binding protein fusion protein that contained the carboxyl-terminal 131 amino acid residues of NHE3 were also tested (Biemesderfer et al., 1997). We were unable to demonstrate cross-reactivity of gill tissue by either western analysis or immunohistochemistry with these three commercially available monoclonal antibodies (Chemicon International, CA, USA).

Cystic fibrosis transmembrane regulator (CFTR)

A commercial monoclonal antibody specific to human CFTR (165–170 kDa) was purchased from NeoMarkers Inc., CA, USA. The antibody was raised against a full-length human CFTR recombinant protein, and the IgM was purified from ascites fluid by ammonium sulphate precipitation (0.2 mg ml^{-1} of 10 mmol l^{-1} PBS, pH 7.4, with 0.2 % bovine serum albumin, BSA, and 15 mmol l^{-1} sodium azide). This antibody did not cross-react with dogfish transmembrane regulator (DFTR) in cryosections and has been reported to cross-react only with human tissue (NeoMarkers Inc.).

Vacuolar-type H^+-ATPase (V-ATPase)

The V-ATPase was immunolocalized using a rabbit polyclonal antibody raised against a synthetic peptide corresponding to a sequence from the catalytic 70 kDa A-subunit of the bovine vacuolar-type H^+-ATPase complex (*C*SHITGGDIYGIVNEN; Südhof et al., 1989) (Protein Service Laboratory, University of British Columbia, Canada). The peptide was conjugated to keyhole limpet haemocyanin using a maleimide linker (Pierce) and mixed (300 μg) with Freund's complete adjuvant (Sigma). New Zealand White rabbits were immunized by subcutaneous injection and boost injections (300 μg) with incomplete Freund's adjuvant followed at biweekly intervals with test bleed. The rabbits were terminally bled and the serum collected. A pre-immunization serum was collected for use as a control. Sera were tested by peptide enzyme-linked immunosorbent assay (ELISA) and western blot analysis of trout gill homogenates.

A polyclonal antibody raised against the same peptide (Südhof et al., 1989) has been used to identify the distribution of the V-ATPase A-subunit in mammalian kidney (Madsen et al., 1991; Kim et al., 1992) and trout gill (Lin et al., 1994). Using rat kidney as a positive control tissue, we found identical results to those cited above.

Carbonic anhydrase

Carbonic anhydrase was immunolocalized using a rabbit polyclonal antibody generated against chick retina carbonic anhydrase II (CAII). The antiserum was kindly provided by P. Linser (The Whitney Laboratory, University of Florida, USA). The antibody cross-reacts strongly with teleost and dogfish erythrocyte and branchial carbonic anhydrase isoforms (Wilson et al., 2000). Western analysis reveals a strong immunoreaction with bands in the 30 kDa molecular mass range.

Immunofluorescence microscopy

Cryosections (5–10 μm) thick were cut on a cryostat at –20 °C, collected onto either 0.01 % poly-L-lysine-coated (Sigma) slides or electrostatically charged slides (SuperFrost Plus, Fisher Scientific) and fixed in acetone at –20 °C for 5 min. Sections were then air-dried. Paraffin sections (5 μm thick) were collected onto charged slides, air-dried at 37 °C overnight, and dewaxed though a series of xylene baths and rehydrated through an ethanol series finishing in PBS. Sections were circled with a hydrophobic barrier (DakoPen, Dako DK) and then blocked with 5 % normal goat serum (NGS)/0.1 % BSA/0.05 % Tween-20 in PBS (TPBS), pH 7.4, for 20 min. Sections were then incubated with primary antibody diluted 1:50 to 1:200 in 1 %NGS/0.1 % BSA/TPBS, pH 7.3, for 1–2 h at 37 °C. They were then rinsed in 0.1 % BSA/TPBS or PBS followed by incubation with goat anti-mouse or anti-rabbit secondary antibody conjugated to fluorescein isothiocyanate (1:50 FITC, Chemicon Intl. Inc.), Texas Red (1:100, Molecular Probes or Jackson Labs) or Cy3

(1:200, Sigma) for 1 h at 37 °C. Following rinsing with 0.1 % BSA/TPBS, sections were mounted with VectaShield mounting medium and viewed on a Zeiss AxioPhot photomicroscope or Bio-Rad 600 confocal microscope with the appropriate filter sets.

To obtain a representative sample, gill tissue from a minimum of 4–6 animals was sectioned and immunolabelled using each of the above-mentioned antibodies. Immunolabelling was repeated on at least on two occasions on slides in duplicate or triplicate for each antibody and animal. Normal mouse or rabbit serum negative controls were also processed at the same time (see below).

Immunoelectron microscopy

Ultrathin sections were prepared on a Reichart ultramicrotome and collected onto either Formvar- or Formvar/carbon-coated nickel grids. Following air-drying, sections were rehydrated by floating the grids on drops of PBS. The grids were then transferred to drops of diluted primary antiserum (1:100) and incubated at room temperature for 1 h. They were then rinsed and transferred to drops of diluted secondary goat anti-mouse antiserum (1:100) conjugated to colloidal gold (10 or 20 nm, Sigma, Chemicon) and incubated for 1 h at room temperature. They were rinsed with PBS and fixed for 10 min in 1 % glutaraldehyde/PBS and rinsed again in double-distilled water before counter-staining with lead citrate and saturated uranyl acetate. Sections were viewed on a Philips 300 transmission electron microscope and photographed with Kodak EM plate film 4489.

SDS–PAGE and western analysis

Tissue was thawed in ice-cold SEI buffer (300 mmol l^{-1} sucrose, 20 mmol l^{-1} EDTA, 100 mmol l^{-1} imidazole, pH 7.3), and filaments were scraped from the arch using a blunt razor blade. Filaments were then homogenized with a Potter–Elvehjem tissue grinder on ice (1000 revs min^{-1}, 10 strokes). The homogenate was centrifuged at 2000 ***g***, and the supernatant was discarded. The pellet was resuspended in 2.4 mmol l^{-1} deoxycholate in SEI buffer and rehomogenized. Following a second centrifugation at 2000 ***g***, the supernatant was saved.

Total protein was measured using the Bradford method (Bradford, 1976) with a BSA standard and the homogenate diluted to 1 μg μl^{-1} in Laemmli's buffer (Laemmli, 1970). Proteins were separated by polyacrylamide gel electrophoresis (PAGE) under denaturing conditions, as described by Laemmli (1970), using a vertical mini-slab apparatus (Bio-Rad, Richmond, CA, USA). Proteins were transferred to Immobilon-P membranes (Millipore) using a semi-dry transfer apparatus (Bio-Rad). Blots were then blocked in 3 % skim milk/TTBS (0.05 % Tween 20 in Tris-buffered saline: 20 mmol l^{-1} Tris-HCl; 500 mmol l^{-1} NaCl, 5 mmol l^{-1} KCl, pH 7.5).

Blots were incubated with primary antiserum for 1 h at room temperature or overnight at 4 °C. Following a series of washes with TTBS, blots were incubated with either goat anti-rabbit or anti-mouse horseradish-peroxidase-conjugated antibody (Sigma). Bands were visualized by enhanced chemiluminescence (Amersham). Tissue homogenates from three animals were electrophoretically separated and probed for each antibody.

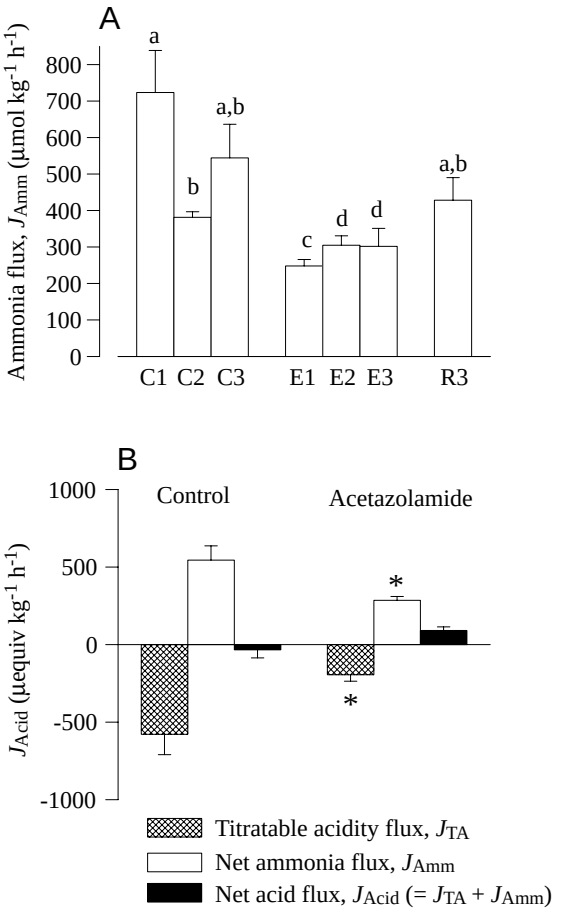

Fig. 1. The effects of the carbonic anhydase inhibitor acetazolamide (0.1 mmol l^{-1}) on (A) net ammonia flux (J_{Amm}; μmol kg^{-1} h^{-1}) and (B) net acid flux (J_{Acid}=J_{TA}+J_{Amm}, where J_{TA} is flux of titratable acidity; μequiv kg^{-1} h^{-1}) in mudskippers in 50 % sea water. The flux series (A) consists of an initial 3 h control period (C1–C3) followed by 3 h exposure (E1–E3) and recovery (R3) periods. J_{Amm} is calculated for each hour during the control and exposure periods and over the entire 3 h period during recovery. In B, J_{Acid} is calculated from the 3 h J_{TA} and J_{Amm} values. Values marked with the same letters in A are not significantly different, and the asterisks in B indicate a significant difference (P<0.05) from the corresponding initial 3 h control value. Note the significant reduction in J_{Amm} following the addition of acetazolamide (B), the recovery of J_{Amm} with time (A) and the absence of changes in J_{acid} (B). Values are means + S.E.M, N=6.

Controls

Normal mouse serum and normal rabbit serum were substituted for primary antibodies in the immunohistochemical and blotting protocols for use as negative controls. Except for the V-ATPase, pre-immune sera were not available. Also, antigens were not available, so pre-absorption controls were also not conducted.

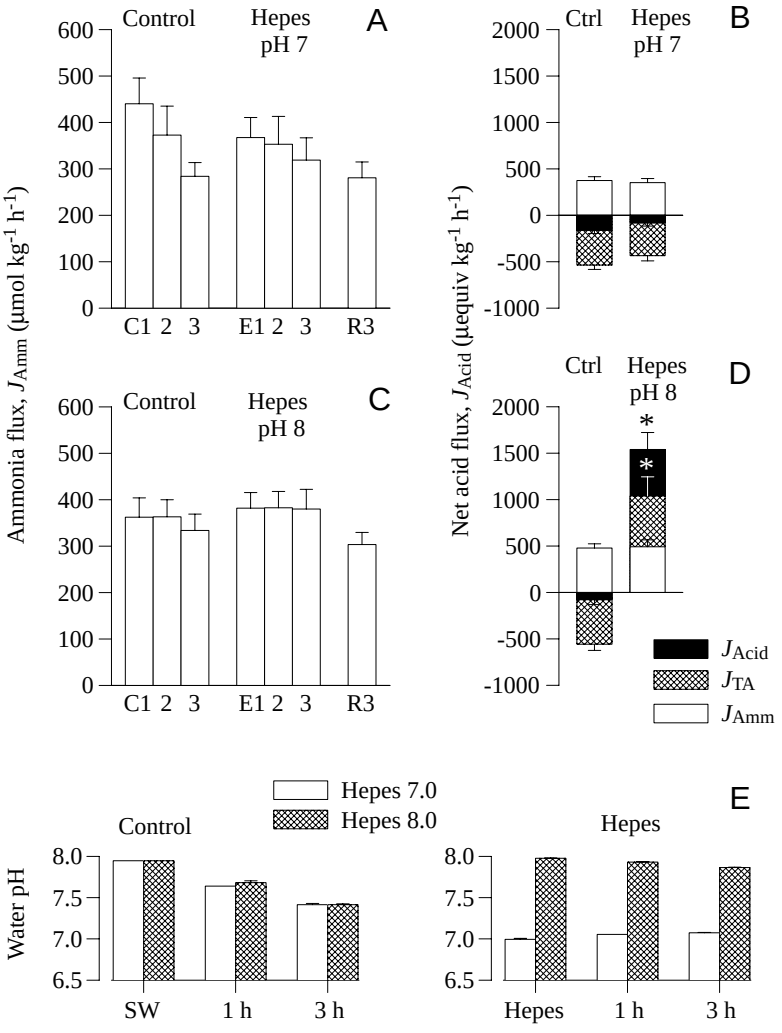

Fig. 2. The effects of changes in boundary-layer pH induced by 5 mmol l^{-1} Hepes, pH 7.0 and pH 8.0, on net ammonia flux (J_{Amm}; μmol kg^{-1} h^{-1}) (A and C respectively) and net acid flux ($J_{Acid}=J_{TA}+J_{Amm}$, where J_{TA} is flux of titratable acidity; μequiv kg^{-1} h^{-1}) (B and D, respectively) in mudskippers in 50 % sea water (SW). The flux series (A,C) consists of an initial 3 h control (Ctrl) period (C1–C3) followed by 3 h exposure (E1–E3) and recovery (R3) periods. J_{Amm} is calculated for each hour during the control and exposure periods and over the entire 3 h period during the recovery. (C,D) J_{Acid} is calculated from the 3 h titratable acidity and J_{Amm} values. The asterisks in D indicate a significant difference ($P<0.05$) from the corresponding initial 3 h control value. (E) Water pH values during the initial 3 h control period and the following 3 h Hepes treatment period at 0, 1 and 3 h. Values are means + S.E.M, N=6.

Statistical analyses

Data are presented as means ± S.E.M. (N). Ammonia excretion rates from the different treatments were compared using a one-way repeated-measures analysis of variance (ANOVA) and *post-hoc* Student–Newman–Keuls test. Net ammonia, titratable acidity and acid fluxes under control and experimental conditions were compared using paired *t*-tests. The fudicial limit of significance was set at 0.05.

Results

Ammonia and acid fluxes

The carbonic anhydrase inhibitor (0.1 mmol l^{-1}) acetazolamide reduces J_{Amm} by 48 % yet has no significant effect on J_{Acid} (Fig. 1). J_{Amm} is inhibited immediately upon exposure to acetazolamide and starts to recover slightly during the second and third hours of exposure. Removal of acetazolamide results in a complete recovery of J_{Amm}.

The addition of 5 mmol l^{-1} Hepes to 50 % sea water is sufficient to fix the water pH at either 7 and 8 during the 3 h experimental period (Fig. 2E). Buffering the water at pH 7.0 does not significantly affect either J_{Amm} or J_{Acid} (Fig. 2A,B). However, addition of 5 mmol l^{-1} Hepes, pH 8, significantly increases J_{Acid} while having no effect on J_{Amm} (Fig. 2C,D).

Immunohistochemistry

Na^+/K^+-ATPase

Figs 3A, 4 and 5A show an abundance of Na^+/K^+-ATPase immunoreactivity associated with the lamellar epithelium. Immunopositive cells are also found in the epithelium of the gill arch. Immunoreactivity for Na^+/K^+-ATPase is restricted to the large epithelial MR cells (Fig. 5A). Labelling occurs throughout the cell body with the exception of the nucleus and apical crypt area. Immunogold labelling for Na^+/K^+-ATPase reveals that the intracellular staining observed by immunofluorescence is restricted to elements of the tubular system and that no labelling is associated with the apical crypt (Fig. 4A,B). Control incubations with normal mouse serum result in negligible levels of immunoreactivity (Fig. 3B). In western blots, the α5 antibody cross-reacts strongly with a band with an apparent molecular mass of 116 kDa (see Fig. 9A).

$Na^+/K^+/2Cl^-$ cotransporter

The $Na^+/K^+/2Cl^-$ cotransporter has an essentially identical

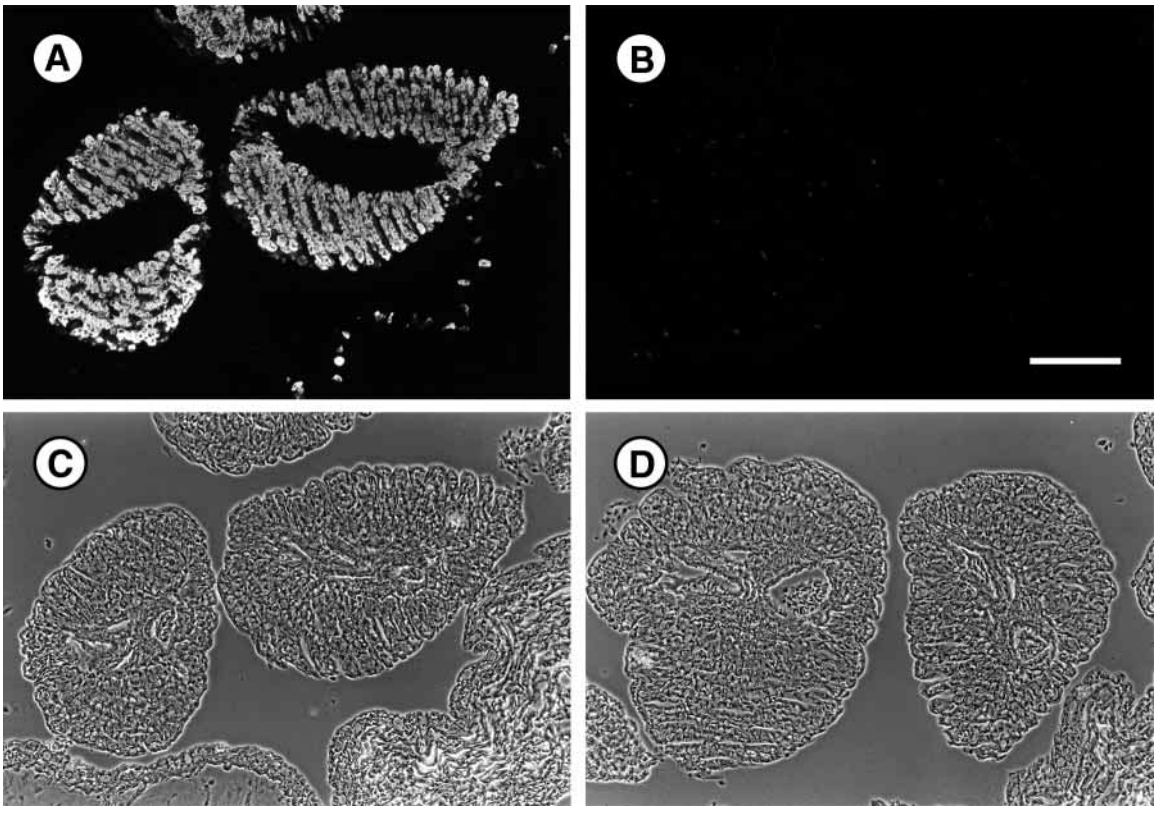

Fig. 3. Indirect immunofluorescence (A) and phase-contrast (C) microscopy showing the distribution of Na^+/K^+-ATPase in the gills of the mudskipper. The mouse monoclonal antibody α5 was used to immunolabel a 5 μm fixed/frozen section of gill tissue fixed in 3 %PFA/PBS (see Materials and methods). In the two gill filaments shown in cross section, staining is most intense in the cells of the gill lamellar epithelium. A section in which α5 was substituted with normal mouse serum in the immunolocalization procedure serves as a control for comparison (B,D). Scale bar, 100 μm.

distribution to that of the Na^+/K^+-ATPase (Fig. 5E,F). $Na^+/K^+/2Cl^-$ immunofluorescence labelling shows a similar diffuse cytoplasmic distribution, and immunogold labelling indicates that the immunoreaction is associated with the MR cell tubular system. No labelling is associated with the apical crypt. We were, however, unable to demonstrate immunoreactivity on western blots using the T4 $Na^+/K^+/2Cl^-$ antibody.

Cystic fibrosis transmembrane regulator

The mouse monoclonal antibody against the human cystic fibrosis transmembrane regulator (CFTR) cross-reacts specifically with the MR cell apical crypt (Fig. 5C,D). In sections, labelled crypts appear as either a ring or a U shape indicative of cross or longitudinal sections through the crypt, respectively. This antibody was only useful with fixed/frozen tissue and not fixed/paraffin-embedded tissue. No immunolabelling is associated with pavement cells, pillar cells, mucocytes, erythrocytes or the basal portion of MR cells. Western blots indicate an immunoreactive band with an apparent molecular mass of 150 kDa (see Fig. 9B).

Na^+/H^+ exchanger

The distributions of apical isoforms of the Na^+/H^+ exchanger (NHE2 and NHE3) were determined in the mudskipper gill using antibodies Ab597 and Ab1380 specific for apical NHE2 and NHE3 isoforms, respectively. Both NHE isoforms are immunolocalized to the apical crypts of MR cells (Figs 6, 7). From low-power photomicrographs, most crypts can be seen to be labelled (Fig. 6A). The NHE3 antibody Ab1381 was not useful for tissue localization. A control incubation with normal rabbit serum reveals non-specific labelling associated with the contents of the afferent and efferent vessels (Fig. 6E). In western blots of crude membrane preparations, immunoreactivity is seen with bands in the predicted molecular mass ranges (approximately 85 kDa); however, additional major bands are also recognized at lower molecular masses (see Fig. 9D,E).

Carbonic anhydrase

Immunoperoxidase staining for carbonic anhydrase in fixed/frozen sections is restricted to the apical crypt region of the MR cells (Fig. 8A,B). Staining is not associated with the rest of the cell. Erythrocytes also show immunoreactivity, while no immunoreactivity is associated with pavement cells or pillar cells. Incubation of control sections with normal rabbit serum at an equivalent dilution results in insignificant levels of labelling.

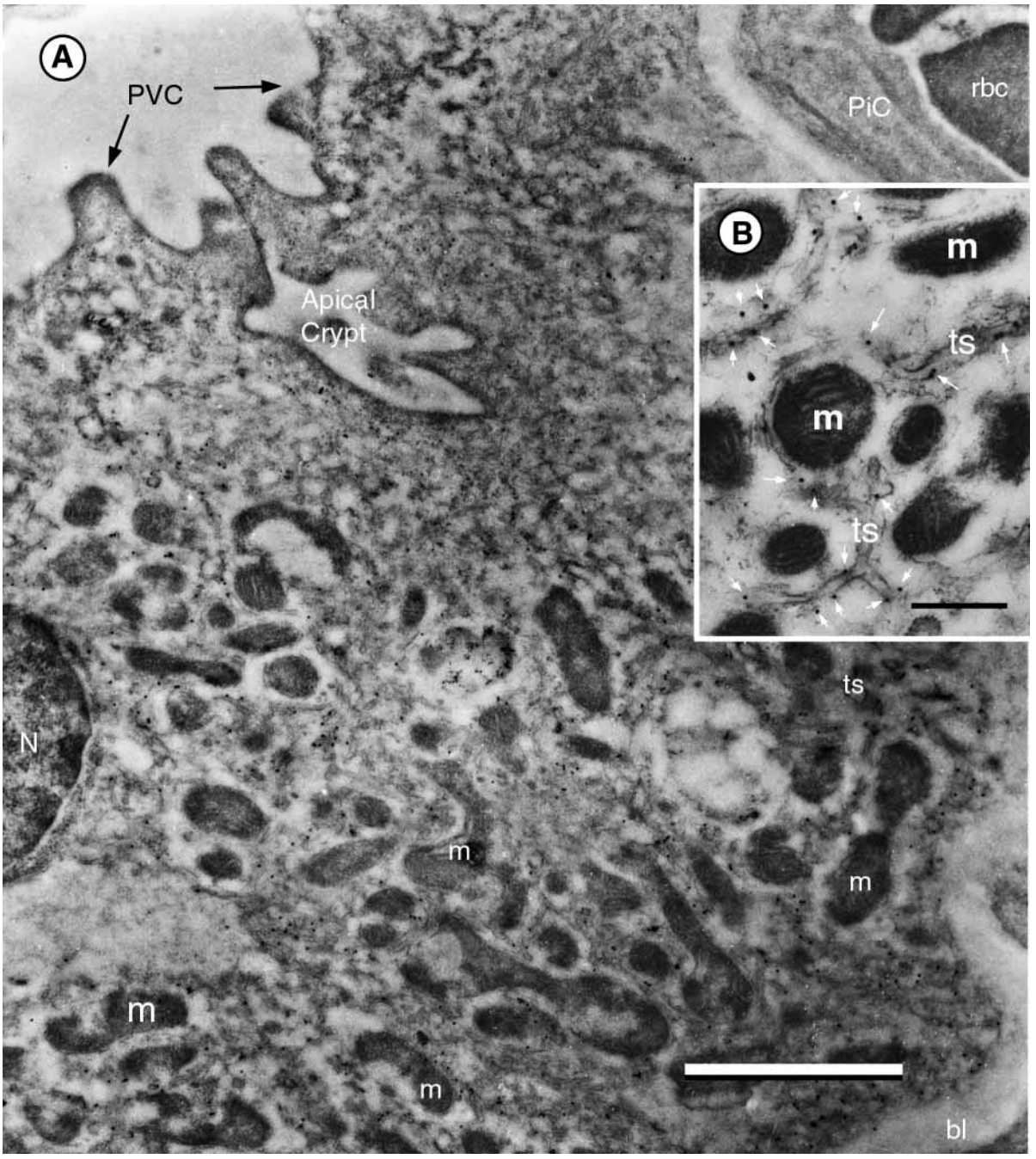

Fig. 4. Immunogold localization of Na^+/K^+-ATPase in the mudskipper gill lamellar mitochondria-rich (MR) cell using the α5 antibody and a secondary antibody conjugated to 20 nm colloidal gold particle. Labelling is greatest in the lower two-thirds of the MR cell (A) and is associated with the tubular system (ts) (B; arrows). No labelling is associated with the MR cell apical crypt, pavement cells (PVC), pillar cells (PiC) or red blood cells (rbc). m, mitochondrion; N, nucleus; bl, basal lamina. Scale bars: A, 2 μm; B, 0.5 μm.

V-ATPase

The V-ATPase was immunolocalized using a polyclonal antibody directed against the A-subunit of the vacuolar proton pump complex. Immunoperoxidase staining shows that the V-ATPase is restricted to the apical crypt region of MR cells (Fig. 8C). It should be noted that some difficulty was encountered in trying to reproduce these results. Western blots show an immunoreactive band with an apparent molecular mass of 78 kDa (Fig. 9C).

Discussion

These results support the hypothesis that, in the amphibious air-breathing mudskipper *Periophthalmodon schlosseri*, ion-

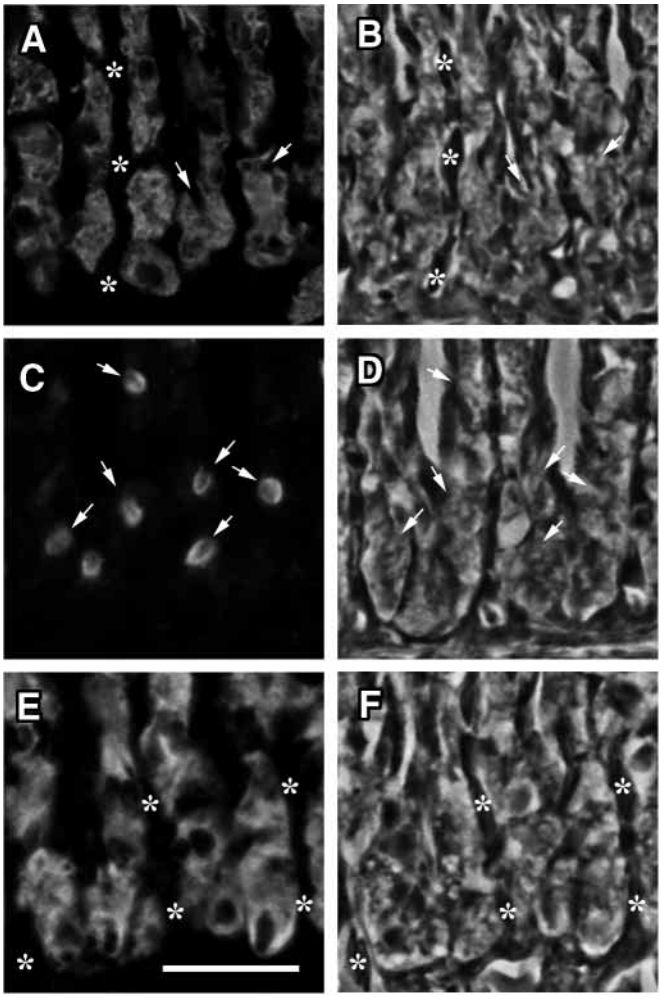

Fig. 5. Indirect immunofluorescence (A,C,E) and phase-contrast microscopy (B,D,F) showing the distributions of Na^+/K^+-ATPase (A,B), the cystic fibrosis transmembrane regulator (CFTR) (C,D) and the $Na^+/K^+/2Cl^-$ cotransporter (E,F) in cells of the lamellar epithelium. Micrographs are taken from the bases of lamellae, and the asterisks indicate the alternating lamellar blood spaces. Arrows indicate the location of mitochondria-rich (MR) cell apical crypts. The Na^+/K^+-ATPase and $Na^+/K^+/2Cl^-$ cotransporter have an essentially identical diffuse cytoplasmic distribution confined to lamellar MR cells. CFTR staining is restricted to the MR cell apical crypt regions. Scale bar, 25 μm

transport proteins in gill MR cells contribute to active ammonia (NH_4^+) excretion. *In vivo* pharmacological studies have shown that a significant proportion of the total ammonia efflux (J_{Amm}) is sensitive to inhibition of the $Na^+/H^+(NH_4^+)$ exchanger by amiloride (Randall et al., 1999) and to inhibition of carbonic anhydrase by acetazolamide (Fig. 1). The elimination of boundary-layer acidification by the addition of 5 mmol l^{-1} Hepes buffer, pH 8.0, to the 50 % sea water was without effect on J_{Amm}, indicating that NH_3 trapping is not an important component of total ammonia excretion (Fig. 2). These animals are also capable of excreting ammonia against inward NH_4^+ and NH_3 gradients (2 mmol l^{-1} NH_4Cl); however, a portion of J_{Amm} is then sensitive to inhibition of $Na^+/K^+(NH_4^+)$-ATPase by ouabain (Randall et al., 1999).

The branchial epithelium contains an abundance of MR cells with deep apical crypts and an extensive tubular system continuous with the basolateral membrane (Wilson et al., 1999). Immunological localization studies have demonstrated the presence of NHE2- and NHE3-like isoforms, a CFTR-like anion channel and carbonic anhydrase associated with the apical crypt and a Na^+/K^+-ATPase and a $Na^+/K^+/2Cl^-$ cotransporter (NKCC) associated with the tubular system of these MR cells. The demonstration of the presence of these transporters within the branchial MR cells strongly indicates that these cells are probably involved in the active elimination of ammonia, although their involvement in active Cl^- elimination (typical of brackish-water teleosts) is also expected (see Marshall and Bryson, 1998).

Boundary-layer acidification

In *P. schlosseri*, excretion of ammonia is not dependent on boundary-layer pH. This would indicate that P_{NH_3} gradients are not as important a mechanism of total ammonia elimination as in freshwater fishes (Cameron and Heisler, 1983; Wilson et al., 1994). The facilitation of NH_3 diffusion by trapping of NH_3 ($NH_3+H^+ \rightarrow NH_4^+$) through the acidification of the boundary layer by hydration of respiratory CO_2 or direct H^+ excretion (by the Na^+/H^+ exchanger or V-ATPase) is important in freshwater fish (Wright et al., 1989; Wilson et al., 1994; Salama et al., 1999) and probably also in seawater fish (Wilson and Taylor, 1992). The mudskippers kept in unbuffered 50 % sea water (pH 8) were able to acidify their bath water to a final pH of approximately pH 7.4 (Fig. 2E). The acidification of the gill boundary layer is dependent on the water buffer capacity. Sea water tends to be poorly buffered, and the gill boundary layer will therefore be acidified. Experimentally, the acidification of the boundary layer can be eliminated by the addition of buffer to the water. In the mudskipper, the elimination of boundary-layer acidification by buffering with 5 mmol l^{-1} Hepes, pH 8.0, results in no change in J_{Amm}. This did, however, stimulate a large J_{Acid}. An increase in J_{Acid} has also been observed in freshwater trout *Oncorhynchus mykiss* (Salama et al., 1999), but not to the same extent.

Ion-transport proteins and elimination of NH_4^+

Na^+/K^+-ATPase and $Na^+/K^+/2Cl^-$ cotransport

The gill MR cells are associated with high levels of Na^+/K^+-ATPase immunoreactivity (Fig. 3), and *in vitro* assays show that (ouabain-sensitive) enzyme activity is also very high, being 3–4 times higher than in another mudskipper species (*Boleophthalmus boddaeti*; Randall et al., 1999). The levels of immunoreactivity in the other gill cell types (pavement cells, erythrocytes, pillar cells, filament-rich cells) are below the level of detection, although the absence of immunoreactivity is not a good criterion for concluding that the enzyme is absent. There are limits to the sensitivity of the technique in addition to the possibility that other isoforms of the α-subunit are present in these cell types. Indeed, Na^+/K^+-

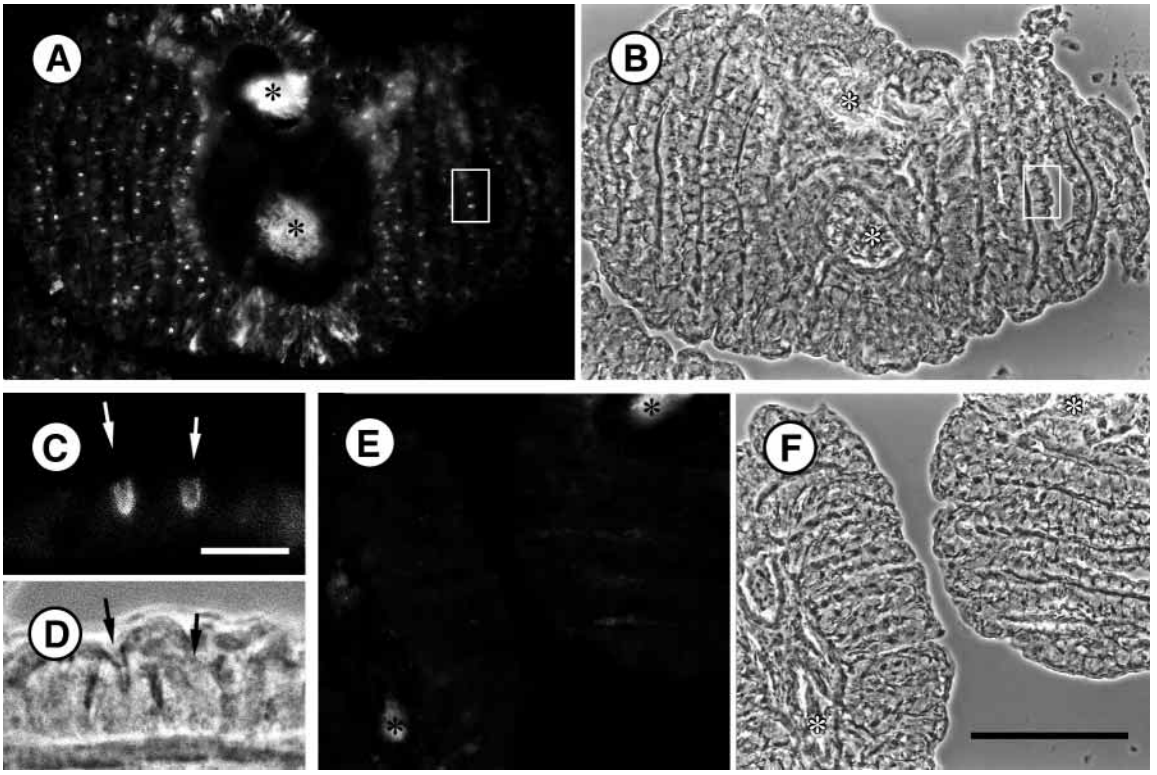

Fig. 6. The distribution of Na^+/H^+ exchanger 3 (NHE3) in the gills of fixed/frozen sections of mudskipper gill demonstrated using indirect immunofluorescence (A,C,E,) and phase-contrast microscopy (B,D,F). The rabbit polyclonal antibody 1380 was used to immunolabel a 5 μm fixed/frozen section of gill tissue fixed in 3% PFA/PBS (see Materials and methods). In low-magnification micrographs, a punctate labelling pattern is associated with the lamellar epithelial cells (A,B). Higher magnification of the boxed areas reveals that this staining is specific for mitochondria-rich (MR) cell apical crypts (C,D; arrows). The asterisks indicate non-specific fluorescence of material associated with the afferent and efferent vessels, as is also evident in the control fluorescence (E) and phase-contrast micrograph (F) pair incubated with normal rabbit serum. Scale bars: A,B,E,F, 100 μm; C,D, 10 μm.

ATPase is probably present in all cell types performing cellular housekeeping roles.

K^+ and NH_4^+ share a similar hydration radius, and NH_4^+ has been shown *in vitro* to compete with K^+ for binding sites on Na^+/K^+-ATPase (Mallery, 1983; Kurtz and Balaban, 1986; Garvin et al., 1985; Towle and Hølleland, 1987; Wall and Koger, 1994) and also on the $Na^+/K^+/2Cl^-$ cotransporter (Kinne et al., 1986). Randall et al. (1999) were able to demonstrate in *P. schlosseri* that physiological levels of NH_4^+ could stimulate the ATPase *in vitro* as well. Only during exposure of these animals to high environmental ammonia levels, when NH_4^+ and NH_3 gradients (2 mmol l^{-1}) are directed inwards, is J_{Amm} sensitive to ouabain. This inhibition of J_{Amm} is associated with a significant increase in plasma ammonia levels (Randall et al., 1999). Thus, in the absence of favourable diffusion gradients NH_4^+ substitution becomes physiologically significant.

Although the $Na^+/K^+/2Cl^-$ cotransporter is found in association with the MR cell tubular system (Fig. 5E) and has been found to substitute NH_4^+ for K^+ in other vertebrates (Kinne et al., 1986), it is not known how significant a contribution this basolateral pathway makes to the net ammonia efflux in the mudskipper. The $Na^+/K^+/2Cl^-$ cotransporter is driven by the Na^+ gradient maintained by the Na^+/K^+-ATPase, and thus $Na^+/K^+/2Cl^-$ cotransport may also only be important when the animal is faced with inward ammonia gradients. Evans et al. (1989) could find no effect of the $Na^+/K^+/2Cl^-$ cotransporter inhibitor bumetanide on ammonia efflux in the Gulf toadfish *Opsanus beta*.

Apical $Na^+/H^+(NH_4^+)$ exchange

The inhibition of the Na^+/H^+ exchanger by amiloride reduces J_{Amm} by 50% (Randall et al., 1999), yet the elimination of boundary-layer acidification is without effect on J_{Amm} (Fig. 2). It seems likely, therefore, that an important component of ammonia elimination is achieved by direct NH_4^+ transport by the Na^+/H^+ exchanger rather than a boundary-layer pH effect on Na^+/H^+ exchange. In renal microvillus membrane preparations, NH_4^+ has been shown to interact with the Na^+/H^+ exchanger (Kinsella and Aronson, 1981; Nagami, 1988; Blanchard et al., 1998).

There are at least five NHE isoforms (NHE1–4 and NHEβ; see Claiborne et al., 1999), although only NHE2 and NHE3 are found apically. Immunoreactivity for both these isoforms is present in the apical crypt of the mudskipper gill MR cells. This contrasts with the finding of NHE3-like cytoplasmic

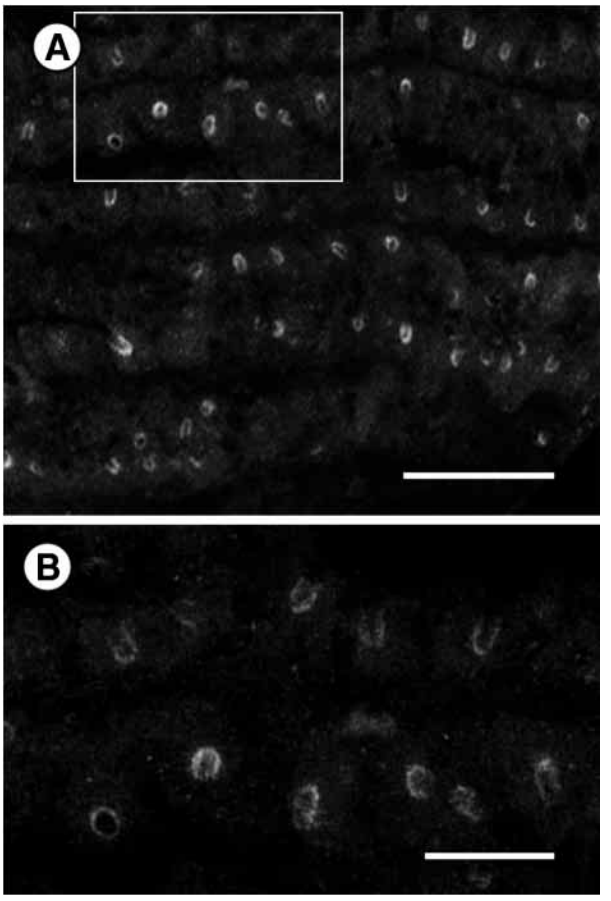

Fig. 7. Projection from a *z*-stack of 50 confocal images (0.2 μm *z*-steps) showing the distribution of Na^+/H^+ exchanger 2 (NHE2) in the gill lamellae of the mudskipper using indirect immunolabelling with the rabbit polyclonal antibody 597. Staining is associated with the apical crypts of lamellar mitochondria-rich (MR) cells and is visible as rings or U-shaped areas of fluorescence. (B) A higher magnification of the area outlined in A. The distribution of NHE2 is essential identical to that of NHE3 demonstrated using antibody 1380 (see Fig. 6). Scale bars: A, 25 μm; B, 10 μm.

immunoreactivity in cells in the filament epithelium of freshwater rainbow trout and seawater wrasse (Edwards et al., 1999). We have observed a similar labelling pattern in tilapia (*Oreochromis mossambicus*) to that reported by Edwards et al. (1999), but with the NHE2 antibody (Wilson, et al., 2000).

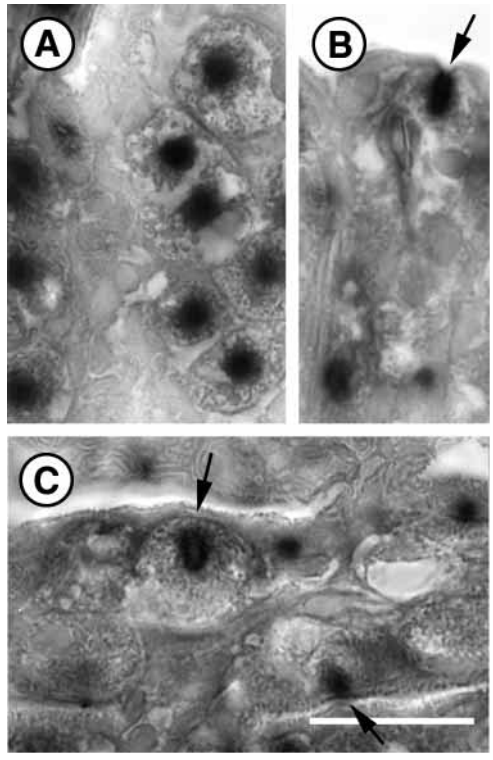

Fig. 8. Indirect immunoperoxidase staining of fixed/frozen sections of gill tissue from the mudskipper. Sections were labelled with antisera to either carbonic anhydrase (A,B) or V-ATPase (C). Intense labelling is associated with the apical crypt region of lamellar mitochondria-rich (MR) cells (arrows). Negligible reactivity was observed in control sections incubated with normal rabbit serum (not shown). Scale bar, 20 μm.

Thus, it would appear that the distribution of the Na^+/H^+ exchanger in the mudskipper is unique amongst teleost fishes.

In the mammalian kidney medulla thick ascending limb, although both isoforms are also present, it is the NHE3 isoform that plays a greater role in ammonium efflux (Paillard, 1998). Recently, Claiborne et al. (1999) have reported the presence of βNHE-like and NHE2-like isoforms in the gill of the sculpin *Myoxocephalus octodecimspinosus* using reverse transcriptase/polymerase chain reaction (RT-PCR). In the marine fish *Opsanus beta*, Evans et al. (1989) found no evidence for apical Na^+/NH_4^+ exchange. Instead, they found

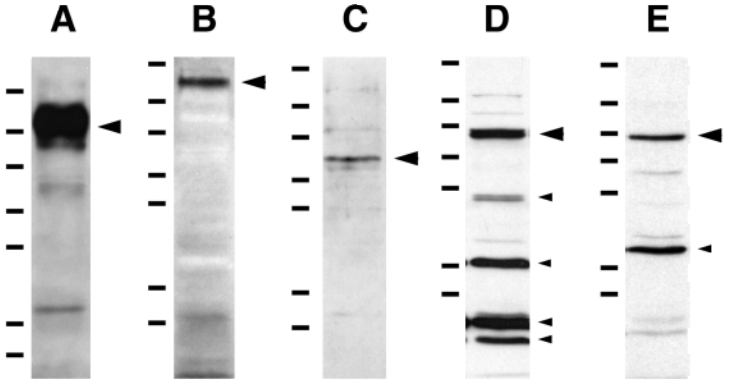

Fig. 9. Western blots of crude homogenates of gill tissue from the mudskipper (10 μg per lane) separated on 10% polyacrylamide gels probed for (A) the α-subunit of Na^+/K^+-ATPase, (B) the cystic fibrosis transmembrane regulator (CFTR) protein, (C) the A-subunit of V-ATPase, (D) Na^+/H^+ exchanger 2 (NHE2) (Ab597) and (E) Na^+/H^+ exchanger 3 (NHE3) (Ab1380). Molecular mass markers: 205, 112, 87, 69, 56, 38.5 and 33.5 kDa (from top to bottom). Large arrowheads indicate bands of interest, and smaller arrowheads indicate other bands.

that total ammonia excretion could be accounted for by non-ionic NH_3 (57 %) and paracellular ionic NH_4^+ (21 %) diffusion and basolateral Na^+/K^+-ATPase activity (22 %). However, their data could be interpreted as indicating that the Na^+/K^+-ATPase and Na^+/H^+ exchange mechanisms are operating in series. Randall et al. (1999) found an increased plasma Na^+ concentration in *P. schlosseri* challenged with high external ammonia levels, which is consistent with the proposed mechanism of Na^+/NH_4^+ exchange.

Carbonic anhydrase

The distribution of carbonic anhydrase in the branchial MR cells is similar to that reported by Lacy (1983) in MR cells from the opercular epithelium of seawater-adapted killifish *Fundulus heteroclitus*. The sensitivity of J_{Amm} to carbonic anhydrase inhibition indicates that intracellular CO_2 hydration maybe important in providing H^+ for NH_3 protonation to maintain P_{NH_3} gradients across the basolateral membrane and in providing NH_4^+ for apical Na^+/NH_4^+ exchange. From the lack of sensitivity of J_{Amm} to ouabain under conditions of low external ammonia concentration (Randall et al., 1999), it would appear that the facilitated movement of NH_4^+ across the basolateral membrane is not important. Amiloride, however, reduced the rate of ammonia excretion in animals in water without any additional ammonia added, indicating that apical Na^+/NH_4^+ exchange may be taking place even when ammonia levels in the water are low.

V-ATPase

Immunoreactivity for the V-ATPase could be demonstrated in the apical crypts of MR cells. However, the role of the V-ATPase in ammonia excretion is not clearly defined in the light of the absence of a pH-dependent boundary-layer effect (Fig. 2) and *in vivo* experiments using KNO_3, which had a delayed effect on J_{Amm} (Randall et al., 1999). The V-ATPase activity observed may only be involved in vesicle acidification (Harvey, 1992).

Cystic fibrosis transmembrane regulator

It was initially thought that the CFTR could be used as a marker for MR cells involved in Cl^- secretion, a function normally ascribed to this cell type in seawater teleost fishes (chloride cells; Marshall and Bryson, 1998; Singer et al., 1998). In the initial investigation of the fine structure of the branchial epithelium, few chloride cell/accessory cell complexes were found, so it was thought that few of the MR cells were actually involved in Cl^- elimination (Wilson et al., 1999). However, CFTR-like immunoreactivity was associated with the apical crypts in almost every branchial MR cell, and it may be that all MR cells are involved in Cl^- elimination. This would be the conclusion if the function of the CFTR were limited to Cl^- conductance; however, the CFTR-like anion channel is also involved in the regulation of other apical channels as well as the conductance of other anions, notably HCO_3^- (Poulsen et al., 1994). The HCO_3^- excretion into the lumen of the duodenum (Hogan et al., 1997) and airways

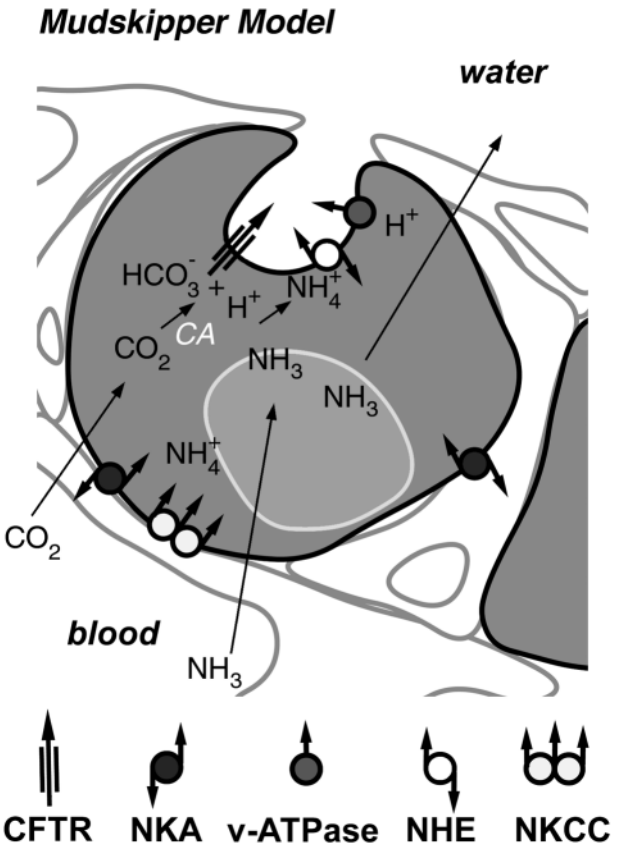

Fig. 10. Illustration of the mudskipper gill mitochondria-rich (MR) cell and its proposed role in active elimination of NH_4^+. Ammonia enters the MR cell from the blood either by diffusion or by active transport by the $Na^+/K^+(NH_4^+)$-ATPase (NKA) and/or the $Na^+/K^+(NH_4^+)/2Cl^-$ cotransporter (NKCC). Intracellular carbonic anhydrase (CA) provides H^+ for NH_3 protonation by catalyzing CO_2 hydration. The NH_4^+ formed is moved across the apical membrane in exchange for Na^+ by a Na^+/H^+ exchange (NHE)-like carrier. The accumulated HCO_3^- exits the cell apically *via* a cystic fibrosis transmembrane regulator (CFTR)-like anion channel.

(M. C. Lee et al., 1998) of mammals is mediated by a CFTR-like anion channel. This latter function becomes quite intriguing. Assuming that CO_2 hydration catalyzed by intracellular carbonic anhydrase provides H^+ for NH_3 protonation to produce NH_4^+ for the Na^+/H^+ exchanger, then a bicarbonate ion is left behind. HCO_3^- must exit the cell across either the basolateral or apical membrane; however, basolateral exit would result in a base load during ammonia excretion. Apical exit facilitated by the CFTR-like channel would be acid–base neutral and would account for the lack of a boundary-layer pH effect. It also explains why J_{Acid} is generally approximately zero and is not affected by the inhibition of J_{Amm} with acetazolamide or amiloride (J. M. Wilson, unpublished observations).

Concluding remarks

Fig. 10 is a model that summarizes our data. The elimination of ammonia by *P. schlosseri* involves a Na^+/H^+ exchanger and

carbonic anhydrase and is not dependent on boundary-layer pH effects. Na^+/K^+-ATPase plays a role in the elimination of ammonia only against an ammonia gradient. Although a V-ATPase and $Na^+/K^+/2Cl^-$ cotransporter are also present, their roles in ammonia elimination are not certain. Immunolocalization studies indicate the presence of all these proteins in the branchial mitochondria-rich cells. It therefore seems reasonable to conclude that these cells are the sites of active elimination of ammonia mediated by ion-transport proteins.

Financial support for this work was provided by NSERC (Canada) and City University of Hong Kong research grants to D.J.R. J.M.W. was supported by UBC graduate fellowships. We would like to thank P. Laurent (CEPE-CNRS), J. Hoffman (IMBC-CNRS) and G. K. Iwama (UBC) for generously providing laboratory space and use of equipment.

References

Biemesderfer, D., Rutherford, P. A., Nagy, T., Pizzonia, J. H., Abu-Alfa, A. K. and Aronson, P. S. (1997). Monoclonal antibodies for high-resolution localization of NHE3 in adult and neonatal rat kidney. *Am. J. Physiol.* **273**, F289–F299.

Blanchard, A., Eladari, D., Leviel, F., Tsimaratos, M., Paillard, M. and Podevin, R.-A. (1998). NH_4^+ as a substrate for apical and basolateral Na^+–H^+ exchangers of thick ascending limbs of rat kidney: evidence from isolated membranes. *J. Physiol., Lond.* **506**, 689–698.

Bradford, M. M. (1976). A rapid and sensitive method for the quantitation of microgram quantities of protein utilizing the principle of protein–dye binding. *Analyt. Biochem.* **72**, 248–254.

Cameron, J. N. and Heisler, N. (1983). Studies of ammonia in the rainbow trout: physico-chemical parameters, acid–base behaviour and respiratory clearance. *J. Exp. Biol.* **105**, 107–125.

Claiborne, J. B., Blackston, C. R., Choe, K. P., Dawson, D. C., Harris, S. P., MacKenzie, L. A. and Morrison-Shetlar, A. I. (1999). A mechanism for branchial acid excretion in marine fish: identification of multiple Na^+/H^+ antiporter (NHE) isoforms in gills of two seawater teleosts. *J. Exp. Biol.* **202**, 315–324.

Edwards, S. L., Tse, C. M. and Toop, T. (1999). Immunolocalization of NHE3-like immunoreactivity in the gills of the rainbow trout (*Oncorhynchus mykiss*) and the blue-throated wrasse (*Pseudolabrus tetrious*). *J. Anat.* **195**, 465–469.

Evans, D. H., More, K. J. and Robbins, S. L. (1989). Modes of ammonia transport across the gill epithelium of the marine teleost fish *Opsanus beta*. *J. Exp. Biol.* **144**, 339–356.

Garvin, J. L., Burg, M. B. and Knepper, M. A. (1985). Ammonium replaces potassium in supporting sodium transport by the Na–K-ATPase of renal proximal straight tubules. *Am. J. Physiol.* **249**, F785–F788.

Harvey, W. R. (1992). Physiology of V-ATPases. *J. Exp. Biol.* **172**, 1–17.

He, X., Tse, C. M., Donowitz, M., Alper, S. L., Gabriel, S. E. and Baum, B. J. (1997). Polarized distribution of key membrane transport proteins in the rat submandibular gland. *Pflügers Arch.* **433**, 260–268.

Hogan, D. L., Crombie, D. L., Isenberg, J. I., Svendsen, P., Schaffalitzky de Muckadell, O. B. and Ainsworth, M. A. (1997). CFTR mediates cyclic AMP- and Ca^{2+}-activated duodenal epithelial HCO_3^- secretion. *Am. J. Physiol.* **272**, G872–G878.

Hoogerwerf, W. A., Tsao, S. C., Devuyst, O., Levine, S. A., Yun, C. H., Yip, J. W., Cohen, M. E., Wilson, P. D., Lazenby, A. J., Tse, C. M. and Donowitz, M. (1996). NHE2 and NHE3 are human and rabbit intestinal brush-border proteins. *Am. J. Physiol.* **270**, G29–G41.

Ip, Y. K., Lee, C. Y., Chew, S. F., Low, W. P. and Peng, K. W. (1993). Differences in the responses of two mudskippers to terrestrial exposure. *Zool. Sci.* **10**, 512–519.

Iwata, K. (1988). Nitrogen metabolism in the mudskipper, *Periophthalmus cantonesis*: Changes in free amino acids and related compounds in various tissues under conditions of ammonia loading, with special reference to its high ammonia tolerance. *Comp. Biochem. Physiol.* **91**A, 499–508.

Iwata, K., Kakuta, I., Ikeda, M., Kimoto, S. and Wada, N. (1981). Nitrogen metabolism in the mudskipper, *Periophthalmus cantonensis*: a role of free amino acids in detoxification of ammonia produced during its terrestrial life. *Comp. Biochem. Physiol.* **68**A, 589–596.

Kim, J., Welch, W. J., Cannon, J. K., Tisher, C. C. and Madsen, K. M. (1992). Immunocytochemical response of type A and type B intercalated cells to increased sodium chloride delivery. *Am. J. Physiol.* **262**, F288–F302.

Kinne, R., Kinne-Saffran, E., Schutz, H. and Scholermann, B. (1986). Ammonium transport in medullary thick ascending limb of rabbit kidney: Involvement of the Na^+,K^+,Cl^--cotransporter. *J. Membr. Biol.* **94**, 279–284.

Kinsella, J. L. and Aronson, P. S. (1981). Interaction of NH_4^+ and Li^+ with the renal microvillus membrane Na^+–H^+ exchanger. *Am. J. Physiol.* **241**, C220–C226.

Kurtz, I. and Balaban, R. S. (1986). Ammonium as a substrate for Na^+–K^+-ATPase in rabbit proximal tubules. *Am. J. Physiol.* **250**, F497–F502.

Lacy, E. R. (1983). Histochemical and biochemical studies of carbonic anhydrase activity in the opercular epithelium of the euryhaline teleost, *Fundulus heteroclitus*. *Am. J. Anat.* **166**, 19–39.

Laemmli, U. K. (1970). Cleavage of structural proteins during the assembly of the head bacteriophage T4. *Nature* **227**, 680–685.

Lee, M. C., Penland, C. M., Widdicombe, J. H. and Wine, J. J. (1998). Evidence that Calu-3 human airway cells secret bicarbonate. *Am. J. Physiol.* **274**, L450–L453.

Lee, M. G., Schultheis, P. J., Yan, Y., Shull, G. E., Bookstein, C., Chang, E., Tse, M., Donowitz, M., Park, K. and Muallem, S. (1998). Membrane-limited expression and regulation of Na^+–H^+ exchanger isoforms by P_2 receptors in the rat submandibular gland duct. *J. Physiol., Lond.* **513**, 341–357.

Lee, T. H., Tsai, J. C., Fang, M. J., Yu, M. J. and Hwang, P. P. (1998). Isoform expression of Na^+–K^+-ATPase α-subunit in gills of the teleost *Oreochromis mossambicus*. *Am. J. Physiol.* **275**, R926–R932.

Levine, S. A., Montrose, M. H., Tse, C. M. and Donowitz, M. (1993). Kinetics and regulation of three cloned mammalian Na^+/H^+ exchangers stably expressed in a fibroblast cell line. *J. Biol. Chem.* **268**, 25527–25535.

Lin, H., Pfeiffer, D. C., Vogl, A. W., Pan, J. and Randall, D. J. (1994). Immunolocalization of proton-ATPase in the gill epithelia of rainbow trout. *J. Exp. Biol.* **195**, 169–183.

Lin, H. and Randall, D. (1991). Evidence for the presence of an

electrogenic proton pump on the trout gill epithelium. *J. Exp. Biol.* **161**, 119–134.

Low, W. P., Ip, Y. K. and Lane, D. J. W. (1990). A comparative study of the gill morphometry in the mudskippers *Periophthalmus chrysospilos*, *Boleophthalmus boddaerti* and *Periophthalmodon schlosseri*. *Zool. Sci.* **7**, 29–38.

Low, W. P., Lane, D. J. W. and Ip, Y. K. (1988). A comparative study of terrestrial adaptations of the gills in three mudskippers, *Periophthalmus chrysospilos*, *Boleophthalmus boddaerti* and *Periophthalmodon schlosseri*. *Biol. Bull.* **175**, 434–438.

Lytle, C., Xu, J. C., Biemesderfer, D. and Forbush III, B. (1995). Distribution and diversity of Na–K–Cl cotransporter proteins: a study with monoclonal antibodies. *Am. J. Physiol.* **269**, C1496–C1505.

Madsen, K. M., Verlander, J. W., Kim, J. and Tisher, C. C. (1991). Morphological adaptation of the collecting duct to acid–base disturbances. *Kidney Int.* **40** (Suppl. 33), S57–S63.

Mallery, C. H. (1983). A carrier enzyme basis for ammnium excretion in teleost gill. NH_4^+-stimulated Na-dependent ATPase activity in *Opsanus beta*. *Comp. Biochem. Physiol.* **74**A, 889–897.

Marshall, W. S. and Bryson, S. E. (1998). Transport mechanisms of seawater teleost chloride cells: An inclusive model of a multifunctional cell. *Comp. Biochem. Physiol.* **119**A, 97–106.

McDonald, D. G. and Wood, C. M. (1981). Branchial and renal acid and ion fluxes in the rainbow trout, *Salmo gairdneri*, at low environmental pH. *J. Exp. Biol.* **93**, 101–118.

McLean, I. W. and Nakane, P. K. (1974). Periodate–lysine–paraformaldehyde fixative. A new fixative for immunoelectron mircoscopy. *J. Histochem. Cytochem.* **22**, 1077–1083.

Morii, H., Nishikata, K. and Tamura, O. (1978). Nitrogen excretion of mudskipper fish *Periophthalmus cantonensis* and *Boleophthalmus pectinirostris* in water and on land. *Comp. Biochem. Physiol.* **60**A, 189–193.

Murdy, E. O. (1989). A taxonomic revision and cladistic analysis of the oxudercine gobies (Gobiidae: Oxudercinae). *Rec. Aust. Mus. Suppl.* **11**, 1–93.

Nagami, G. T. (1988). Luminal secretion of ammonia in the mouse proximal tubule perfused *in vitro*. *J. Clin. Invest.* **81**, 159–164.

Paillard, M. (1998). H^+ and HCO_3^- transporters in the medullary thick ascending limb of the kidney: molecular mechanisms, function and regulation. *Kidney Int.* **53**, S36–S41.

Peng, K. W., Chew, S. F., Lim, C. B., Kuah, S. S. L., Kok, W. K. and Ip, Y. K. (1998). The mudskippers *Periophthalmodon schlosseri* and *Boleophthalmus boddaerti* can tolerate environmental NH_3 concentrations of 446 and 36 mM, respectively. *Fish Physiol. Biochem.* **19**, 59–69.

Philpott, C. W. (1980). Tubular system membranes of teleost chloride cells: osmotic response and transport sites. *Am. J. Physiol.* **238**, R171–R184.

Pisam, M. (1981). Membranous systems in the 'chloride cell' of teleostean fish gill; their modifications in response to the salinity of the environment. *Anat. Rec.* **200**, 401–414.

Pisam, M. and Rambourg, A. (1991). Mitochondria-rich cells in the gill epithelium of teleost fishes: An ultrastructural approach. *Int. Rev. Cytol.* **130**, 191–232.

Poulsen, J. H., Fischer, H., Illek, B. and Machen, T. E. (1994). Bicarbonate conductance and pH regulation capability of cystic fibrosis transmembrane conductance regulator. *Proc. Natl. Acad. Sci. USA* **91**, 5340–5344.

Randall, D. J., Wilson, J. M., Peng, K. W., Kok, W. K., Kuah, S. S. L., Chew, S. F., Lam, T. J. and Ip, Y. K. (1999). The mudskipper, *Periophthalmodon schloesseri*, actively transports NH_4^+ against a concentration gradient. *Am. J. Physiol.* **277**, R1562–R1578.

Randall, D. J., Wood, C. M., Mommsen, T. P., Perry, S. F., Bergman, H., Maloiy, G. M. O. and Wright, P. A. (1989). Urea excretion as a strategy for survival in a fish living in a very alkaline environment. *Nature* **337**, 165–166.

Saha, N. and Ratha, B. K. (1990). Alterations in excretion pattern of ammonia and urea in freshwater air-breathing teleost, *Heteropneustes fossilis* (Boch) during hyperammonia stress. *Indian J. Exp. Biol.* **28**, 597–599.

Salama, A., Morgan, I. J. and Wood, C. M. (1999). The linkage between Na^+ uptake and ammonia excretion in rainbow trout: kinetic analysis, the effects of $(NH_4)_2SO_4$ and NH_4HCO_3 infusion and the influence of gill boundary layer pH. *J. Exp. Biol.* **202**, 697–709.

Schöttle, E. (1931). Morphologie und Physiologie der Atmung bei wasser-, schlamm- und landlebenden Gobiiformes. *Z. Wiss. Zool.* **140**, 1–114.

Singer, T. D., Tucker, S. J., Marshall, W. S. and Higgins, C. F. (1998). A divergent CFTR homologue: highly regulated salt transport in the euryhaline teleost *F. heteroclitus*. *Am. J. Physiol.* **274**, C715–C723.

Südhof, T. C., Fried, V. A., Stone, D. K. and Johnston, P. A. (1989). Human endomembrane H^+ pump strongly resembles the ATP-synthetase of *Archaebacteria*. *Proc. Natl. Acad. Sci. USA* **86**, 6067–6071.

Sun, A. M., Liu, Y., Dworkin, L. D., Tse, C. M., Donowitz, M. and Yip, K. P. (1997). Na^+/H^+ exchanger isoform 2 (NHE2) is expressed in the apical membrane of the medullary thick ascending limb. *J. Membr. Biol* **160**, 85–90.

Takeyasu, K., Tamkun, M. M., Renaud, K. J. and Fambrough, D. M. (1988). Ouabain-sensitive $(Na^+ + K^+)$-ATPase activity expressed in mouse L cells by transfection with DNA encoding the α-subunit of an avian sodium pump. *J. Biol. Chem.* **263**, 4347–4354.

Towle, D. W. and Hølleland, T. (1987). Ammonium ion substitutes for K^+ in ATP-dependent Na^+ transport by basolateral membrane vesicles. *Am. J. Physiol.* **252**, R479–R489.

Tse, C. M., Levine, S. A., Yun, C. H., Khurana, S. and Donowitz, M. (1994). Na^+/H^+ exchanger-2 is an O-linked but not an N-linked sialoglycoprotein. *Biochemistry* **33**, 12954–12961.

Verdouw, H., van Echeld, C. J. A. and Dekkers, E. M. J. (1978). Ammonia determination based on indophenol formation with sodium salicylate. *Water Res.* **12**, 399–402.

Wall, S. M. and Koger, L. M. (1994). NH_4^+ transport mediated by Na^+–K^+-ATPase in rat inner medullary collecting duct. *Am. J. Physiol.* **267**, F660–F670.

Wilson, J. M., Kok, W. K., Randall, D. J., Vogl, A. W. and Ip, Y. K. (1999). Fine structure of the gill epithelium of the terrestrial mudskipper, *Periophthalmodon schlosseri*. *Cell Tissue Res.* **298**, 345–356.

Wilson, J. M., Laurent, P., Tufts, B. L., Benos, D. J., Donowitz, M., Vogl, A. W. and Randall, D. J. (2000a). NaCl uptake by the branchial epithelium in freshwater teleost fish: an immunological approach to ion-transport protein localization. *J. Exp. Biol.* **203**, 2279–2296.

Wilson, J. M., Randall, D. J., Vogl, W. A., Harris, J. Sly, W. S. and Iwama, G. K. (2000b). Branchial carbonic anhydrase is present in a shark, *Squalus acanthias*. *Fish Physiol. Biochem.* (in press).

Wilson, R. W. and Taylor, E. W. (1992). Transbranchial ammonia gradients and acid–base responses to high external ammonia

concentration in rainbow trout (*Oncorhynchus mykiss*) acclimated to different salinities. *J. Exp. Biol.* **166**, 95–112.

Wilson, R. W., Wright, P. M., Munger, S. and Wood, C. M. (1994). Ammonia excretion in freshwater rainbow trout (*Oncorhynchus mykiss*) and the importance of gill boundary layer acidification: lack of evidence for Na^+/NH_4^+ exchange. *J. Exp. Biol.* **191**, 37–58.

Witters, H., Berckmans, P. and Vangenechten, C. (1996). Immunolocalization of Na^+,K^+-ATPase in the gill epithelium of rainbow trout, *Oncorhynchus mykiss*. *Cell Tissue Res.* **283**, 461–468.

Wright, P. A., Randall, D. J. and Perry II, S. F. (1989). Fish gill water boundary layer: a site of linkage between carbon dioxide and ammonia excretion. *J. Comp. Physiol.* **158**, 627–635.